Numerical Heat Transfer Analysis of a Flat Plate using Combined Jet Impingement and Film cooling, with Flow Patterns

Mr. Deepak Raj P.Y
Department of Aeronautical Engineering, Srinivas Institute of Technology, Valachil, Mangaluru

Prof. Devaraj. K
Department of Mechanical Engineering, BMS college of Engineering, Bengaluru

Abstract

Jet Impingement is the most commonly used methods of cooling of gas turbine blades. This is often combined with film cooling to further increase the cooling performance. Adiabatic flow and thermal calculations are carried out by using shear stress transport (SST) k-ω and standard k-ε turbulence model. The coolant-mainstream interactions in the presence of impingement and film cooling are described. Due to the combined effect of impingement and film cooling, the target surface is cooled effectively. Adiabatic heat transfer permits a significant reduction in the time required to generate the mesh and cost. As the blowing ratio increases from 0.6 to 2.4, the local streamwise effectiveness values show an increasing trend and also causes jet-lift-off. A good flow structure is responsible for the increase in effectiveness.

Keywords: *Film cooling, Combined impingement and film cooling, Adiabatic heat transfer, CFD.*

1. Introduction

A gas turbine blade is protected by several cooling schemes to ensure the blade temperature and thermal stresses within safe limits. Among them, film and impingement cooling are frequently used. From the literature the gas turbine blades are cooled by impingement with film cooling holes (effusion holes) which gives a combination of cooling both inner and outer surfaces. The previous researchers have investigated these techniques individually and reported their merits and demerits. The combined effect of impingement and film cooling schemes are the latest to be reported by the investigator and sparse in nature.

Rajesh Kumar Panda and B.V.S.S.S Prasad [1] conducted computational and experimental studies on a flat plate for the combined impingement and film cooling configurations and reported that the effectiveness would increase with blowing ratio due to the enhancement in both impingement and film cooling. Chougule N.K et al. [2] conducted CFD analysis of multi-jet impingement on flat plate and reported that shear stress transport (SST) k-□ turbulence model can give the better predictions of fluid flow and heat transfer properties. Ashok Kumar. M and B.V.S.S.S Prasad [3] computationally studied the flow and heat transfer from staggered multiple circular air jets impinging on a flat surface with effusion holes and primary vortices forming up-wash region and secondary vortices forming a secondary stagnation zone are predicted. B. A. Haven and M. Kurosaka [4] experimentally studied the kidney and anti-kidney vortices in crossflow jets and reported that the counter-rotating vortices relative to one another affects both the lift-off of the jet and the entrainment of crossflow fluid toward the plate surface. Mahmood Silieti et al. [5] compared the effect of the conjugate and adiabatic heat transfer on the film cooling effectiveness using CFD models and reported that conjugate heat transfer models predicts a significant difference in the temperature predictions in comparison with the adiabatic models.

The present computational study was conducted to investigate the effect of the presence of impingement cooling on the effectiveness of film cooling holes. It is evident from the above literature that no systematic comparison of flow and heat transfer characteristics and cooling effectiveness is available for the combined impingement and film cooling configurations under adiabatic thermal conditions. This technique would greatly help in determining if any impingement pattern

IJERT

is implemented on the coolant side how it would affect the film cooling effectiveness. So this makes the problem statement. This study also gives a broader view to look at optimization of the impingement and film cooling holes pattern while designing a cooling system. However the level of assumptions and actual contribution towards this research are need to be developed and to be understood fully, which shall guide and set a clear benchmark to start the current work.

2. Computational Methodology

2.1. Physical Model

The physical model for the present computational study mimics the experimental setup used by Rajesh Kumar Panda and B.V.S.S.S. Prasad [1]. Accordingly, experiments are performed with typical geometric configuration with multiple staggered rows of cylindrical film holes having a length to diameter ratio of four and inclined at 35° streamwise to the surface, and a 14 x 14 matrix of impingement holes. Figure 1 shows the schematic diagram of impingement and target plate.

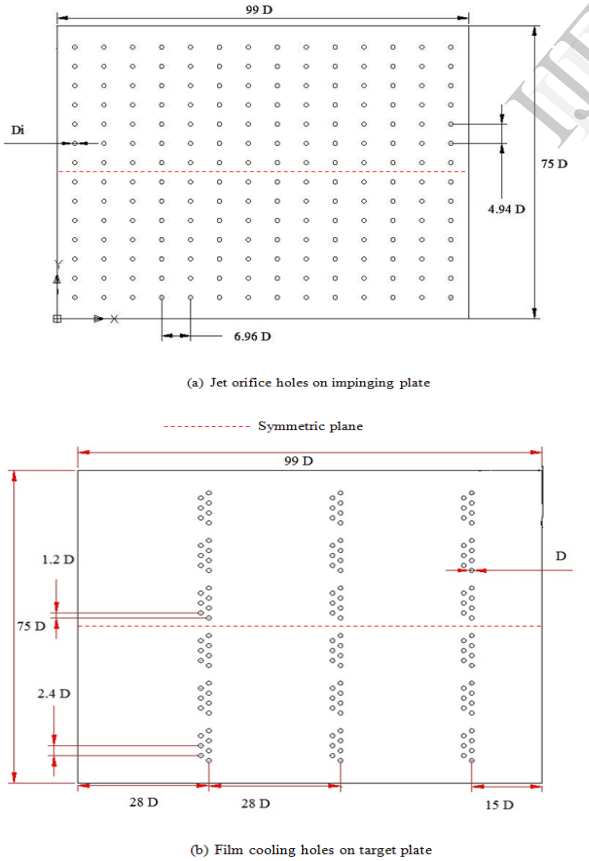

Figure 1. Schematic diagram of impingement and target plate

Table 1. Geometrical details of test section used in experimental setup

DIMENSION	VALUE
Jet orifice (Impingement hole) diameter(D_i)	5.25 mm
Cylindrical Film hole diameter (D)	5 mm
Impinging plate thickness	4 mm
Target plate thickness	12.3 mm
Length to diameter ratio of the film hole	4
Height of the jet orifice from the target surface, (H/D)	1.26

2.2. Computational Domain and Mesh

Figure 2 shows the computational domain that mimics the physical model. The domain consists of hot mainstream path, coolant flow path and solid plate with film holes. The hot mainstream air passes through the test section with a specified uniform velocity and temperature conditions at the inlet and a specified value of atmospheric pressure at the exit. Uniform values of inlet velocity and temperature are specified in the entrance of impingement hole. The impingement chamber is closed from all the sides and hence the coolant passes out only through the cylindrical film holes. The coolant comes out through the film holes and interacts with the mainstream. The present model is symmetric about the plane shown in Figure 1. This symmetry condition helps in reducing the computational efforts.

The computational model and mesh suitable for finite volume method is generated by pre-processor ANSYS ICEM CFD 14.5. Unstructured tetrahedral mesh is generated for the fluid domain which allows greater flexibility, time saving and easy adaptation. A fine cluster of mesh is generated close to the near-wall regions and in the vicinity of the injection holes.

The first cell adjacent to the wall is at a distance that will yield a y^+ value less than 2; as this is a requirement for most turbulence models. Non-uniform grids with clustered nodes are generated in the regions where steep gradient of temperature is expected. Grid independence study is done by analysing the variation of temperature along the X/D for one blowing ratio 0.6. From figure 3 is seen that, there is no change in temperature distribution along X/D for 3.6 million and

IJERT

4.2 million mesh. To get the advantage of computational time 3.6 million mesh is used in this case.

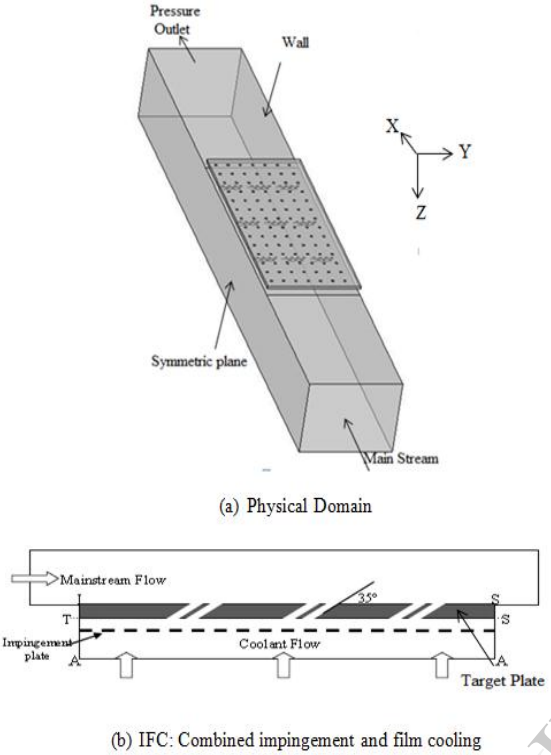

Figure 2. Computational domain with boundary condition

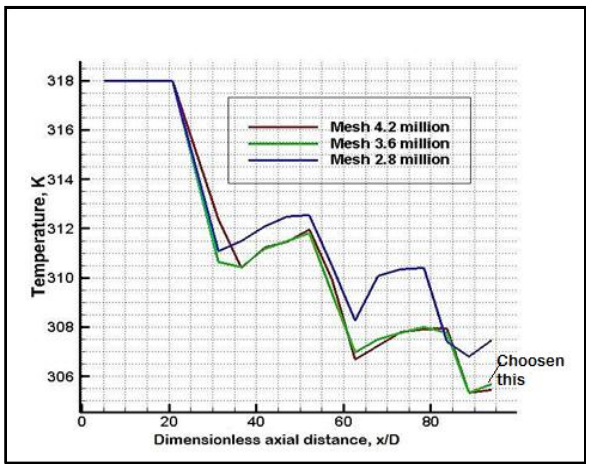

Figure 3. Temperature distribution along X/D for various mesh for M=0.6

2.3. Numerical Simulation

Three dimensional steady state simulations are carried out by using commercial finite volume based software package solver ANSYS FLUENT 14.5.
Assumption made:

- The fluid is incompressible.
- Constant fluid properties.
- Radiation and natural convection are neglected.
- Viscous dissipation is absent and
- The flow is steady.

The governing equations used for the simulation are: the continuity, the momentum and the energy equations along with the equations for turbulence quantities which are described in chapter 4. As both impingement and film cooling are present, the different turbulence model cases i) SST k-ω and ii) k-ε model is adopted for simulation. SIMPLE algorithm is used for pressure velocity coupling. The standard interpolation scheme is used for pressure. The second order upwind scheme is used for momentum and energy and first order upwind scheme is used for turbulent kinetic energy and specific dissipation rate.

The solution is considered to be converged when the maximum residual value is in the order of 10^{-4} for continuity, and 10^{-6} for the momentum, turbulence quantities and for the energy equation. Further, the net results of Mass flow rate in flux reports gives -2.272 x 10^{-7} for 2000 consecutive iterations.

5.4 Boundary Condition

Boundary conditions are applied to the computational model based on the data collected from the experiment. The boundary conditions used for the present study are as follows:

i) Uniform inlet velocity is considered both for main stream and coolant
ii) The exit pressure is set to atmospheric
iii) No slip condition on wall

Reynolds number (based on impingement hole diameter, $\left(\frac{\rho V_{oe} D_i}{\mu}\right)$) at the impingement hole exit is kept constant at 825. The turbulence intensity and turbulent length scale at the mainstream inlet boundary are 1% and 10% of the hydrodynamic diameter, respectively. The turbulence intensity and length scale at inlet boundary of coolant are 1% and diameter of the film hole respectively. Details of the boundary condition are given in Table 2.

4. Validation

The present study is validated by comparing the temperature distribution along the dimensionless axial distance, x/D with the experimental data of Rajesh Kumar Panda and B.V.S.S.S. Prasad [1]. Among various turbulence models available in the Fluent code, standard *K*-ε, and *SST-K*-ω models are tested. The case

IJERT

with blowing ratio M=0.8 is considered for comparison. Figure 4 shows the measured data of [1] and the computed temperature variation from the present study with the two turbulence models. It is observed that k-ε model over predicts the temperature value whereas SST k-ω model's prediction is much better. The agreement between the measured and computational data from SST k-ω is within +8% of total temperature difference, because of adiabatic heat transfer the computational results will not match with experimental. From above discussions it is clear that *K-ω-SST* model predicts the heat transfer better than the other models and hence all the following results are reported with the *K-ω-SST* model. This gives a confidence to the present computational procedure.

Table 2. Details of input condition for IFC

M	V_m (m/s)	T_m (K)	T_c (K)	V_{oe} (m/s)
0.6	4.5	318	303	2.7
0.8	3.375	318	303	2.7
1.0	2.7	318	303	2.7
1.6	1.7	318	303	2.7
2.0	1.35	318	303	2.7
2.4	1.125	318	303	2.7

5. Results and Discussion

5.1. Structure of Flow and Temperature Distributions

Figure 5 and 6 shows the temperature variation for combined impingement and film cooling. From this plot it is clear that by the combination of impingement and film cooling, the target plate is effectively cooled.

The effect of Blowing ratios studied by increasing from M = 0.6 to M = 2.4 and the results are obtained as temperature contours which are varied along the x-coordinate, the variation of temperature in x-z plane for different Blowing ratio are shown in figure 7. From this plot it is clear that as blowing ratio increases, coolant will lift off from the surface, so proper cooling will not take place and also disturbs the boundary layer. The Figure 7 also shows coolant quickly increases in temperature as it flows downstream.

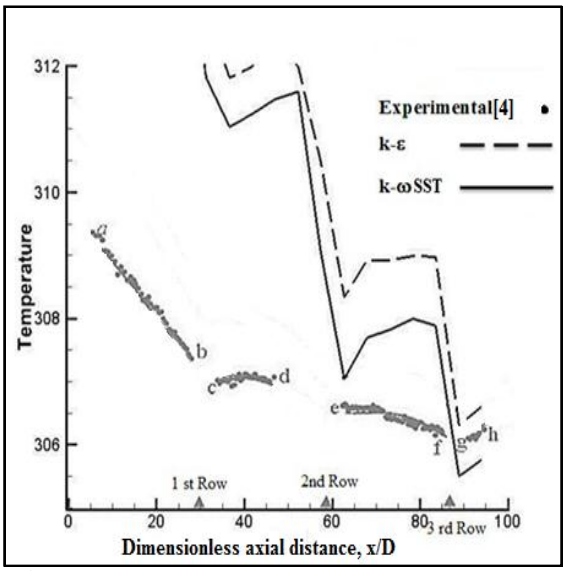

Figure 4. Comparison of Temperature variation along Dimensionless axial distance, X/D for M=0.8 with Rajesh Kumar Panda and B.V.S.S.S. Prasad [1] experimental data

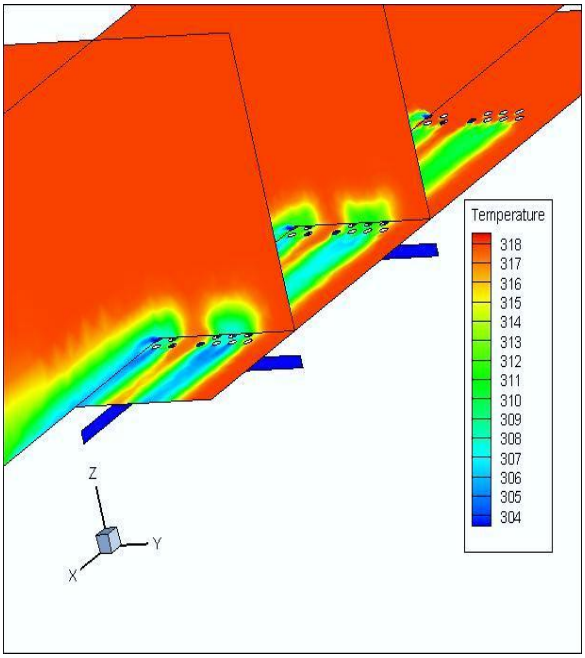

Figure 5 Temperature distribution on target plate for the combined impingement and film cooling over entire domain.

IJERT

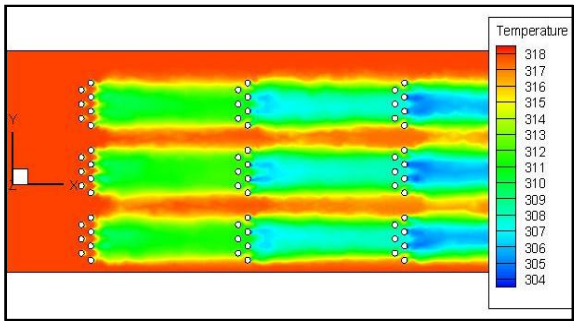

Figure 6. Temperature distribution on target plate for the combined impingement and film cooling over the target plate.

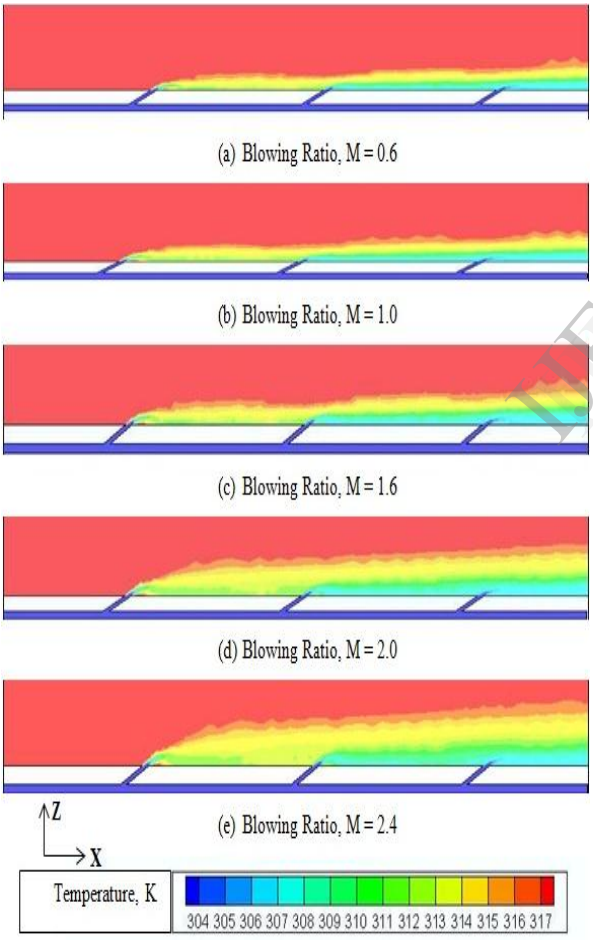

Figure 7. Temperature variation on target plate for different blowing ratio from M=0.6 to M=2.4.

Figure 8 reveals the essential differences of flow over target surface are plotted by the help of stream traces.

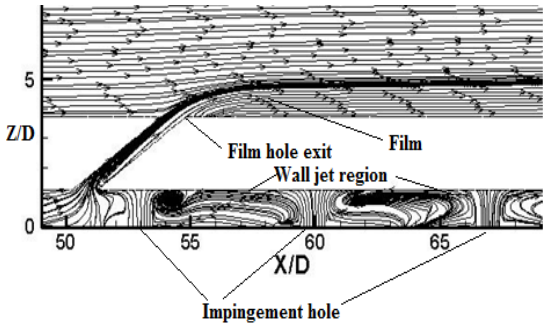

Figure 8. Streamlines of impingement-film cooling configuration for M = 0.6

Figure 8 and 9 show the stream traces for the cases with impingement-film cooling configurations. It can be seen impinging jets form a stagnation zone of impingement location and then forms a wall jet region where boundary layer starts developing. Adjacent jets interact and produce an up wash flow surrounded by counter rotating vortices as shown figure 9 (a). It is seen that the boundary layer developed in the wall jet region is removed due to suction created by the film holes. This boundary layer removal increases the heat transfer to a reasonable value. Here as the H/D ratio is small, it is unable to differentiate the potential core and free jet region. The flow separation near to film hole entry and exit can be easily visualized. This flow separation increases the velocity of coolant and decreases the pressure over the vicinity of film cooling so that which helps in cooling of target surface. The combination of impingement and film cooling take the advantages of both impingement and film cooling, so that we are able to achieve effective cooling. The lift-off of the coolant can be easily visualized and compared with the figure 9.

The lowest blowing ratio provides lowest heat-transfer enhancement. With increase in blowing ratio, the heat transfer coefficient increases for x/D locations. Minimum heat transfer coefficients are found at medium blowing ratios. Figure 10 shows the exit temperature profiles in term of dimensional temperature of the coolant for IFC configurations with different blowing ratios. It is evident that the exit temperature is more uniform for impingement-film cooling configuration.

In the figure 10, there is a sudden temperature variation in the position of film rows. As the distance increases from the film hole the temperature decreases and quickly increases in temperature as it flows downstream. From this for low blowing ratio cooling of target surface is more than the high blowing ratio.

IJERT

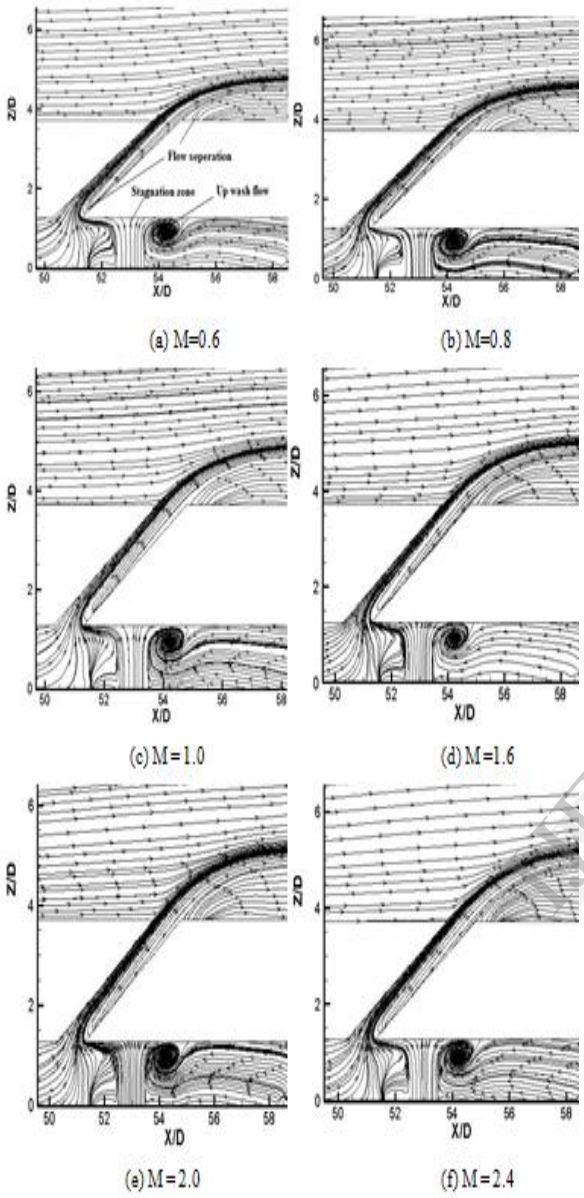

Figure 9. Streamlines of impingement-film cooling configurations for different blowing ratio from 0.6 to 2.4

Figure 11 shows the comparison of the effectiveness values for impingement-film cooling configuration for six blowing ratios. As the plate is cooled, the temperature decreases along the plate and hence the effectiveness increases for impingement-film cooling configuration due to the effect of high impingement heat transfer coefficient. This difference in values is noticed all along the stream wise direction. Effectiveness decreases significantly with increasing blowing ratio as shown in figure 11. High effectiveness values are obtained immediately downstream of the holes and decrease rapidly downstream.

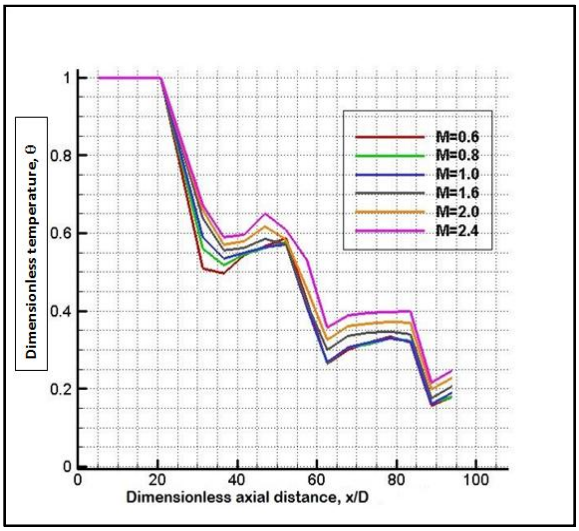

Figure 10. Dimensionless temperature variation along the dimensionless axial distance for varying M for IFC configuration

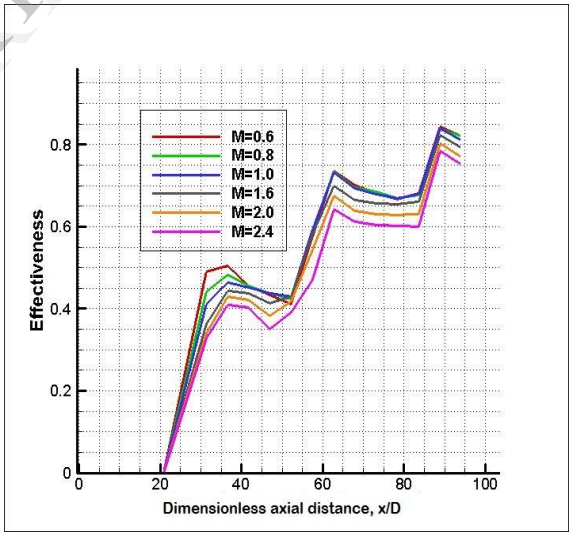

Figure 11. Comparison of effectiveness for different blowing ratios

5.2. Coolant-Mainstream Interactions

As the coolant exits from the film hole as a jet it interacts with the hot mainstream starting from the leading edge of the hole. The resulting flow structure is three dimensional in nature and its structure differs significantly at various downstream locations. In order to present the variations of the flow and temperature patterns and effectiveness distribution on the interaction surface, six typical transverse planes are chosen at different axial distances as shown in figure

IJERT

12. Among these, planes U1, U2 and U3 chosen at the leading edge of the first, second and third row holes respectively. Planes D11, D12 andD13 are located at two, ten and eighteen film hole diameters downstream from the trailing edge of the first row.

Figure 13 shows the stream traces (projection of flow lines of the predicted velocity field on the y-z plane) across these six transverse planes and for six blowing ratios. The projection of flow lines on a y-z plane are obtained from the v and w components of the velocity vectors on that plane. The nodal points of attachment (N) are formed where all stream lines are directed outward in plane U1, signifying the distance up to which the mainstream gets deflected by the coolant jet at the leading edge. This distance is called jet-lift-off, which increases with increasing blowing ratios.

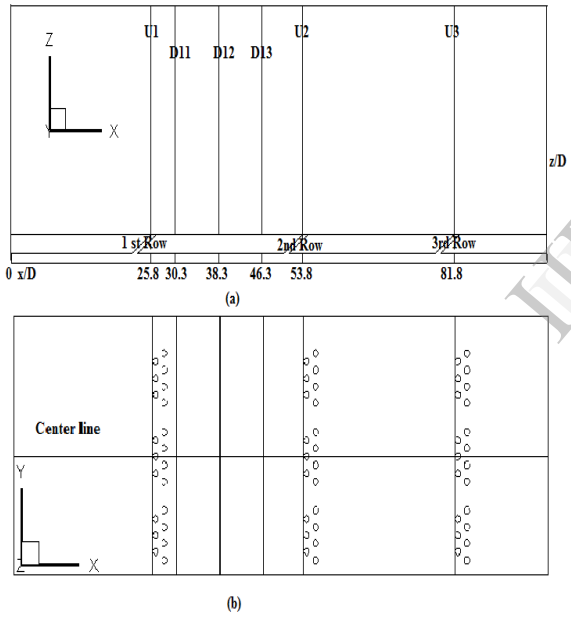

Figure 12. Data reduction Planes, (a) Front view and (b) top view

The lift-off phenomenon is also evident in figure 8 and 9. As the jet exits from the film hole it covers part of the downstream region. However, the flow from the side hole of the same row and the mainstream prevent it from further spreading. The complex interactions between these fluids lead to the formation of counter rotating vortex pair. It is observed from this figure that the streamwise vortices comprise of more than single set of counter-rotating vortex pair. If two interacting vortices, with same sense of rotation add together each other, lift-off is promoted [4].At plane D11 the counter rotating vortices are aided as shown in figure 13 (b), and at plane D12 and D13 they are dissipated as in figure 13 (c) and (d).

The corresponding stream traces further downstream in planes U2 and U3 show the important difference of the incoming flow structure with different blowing ratios.

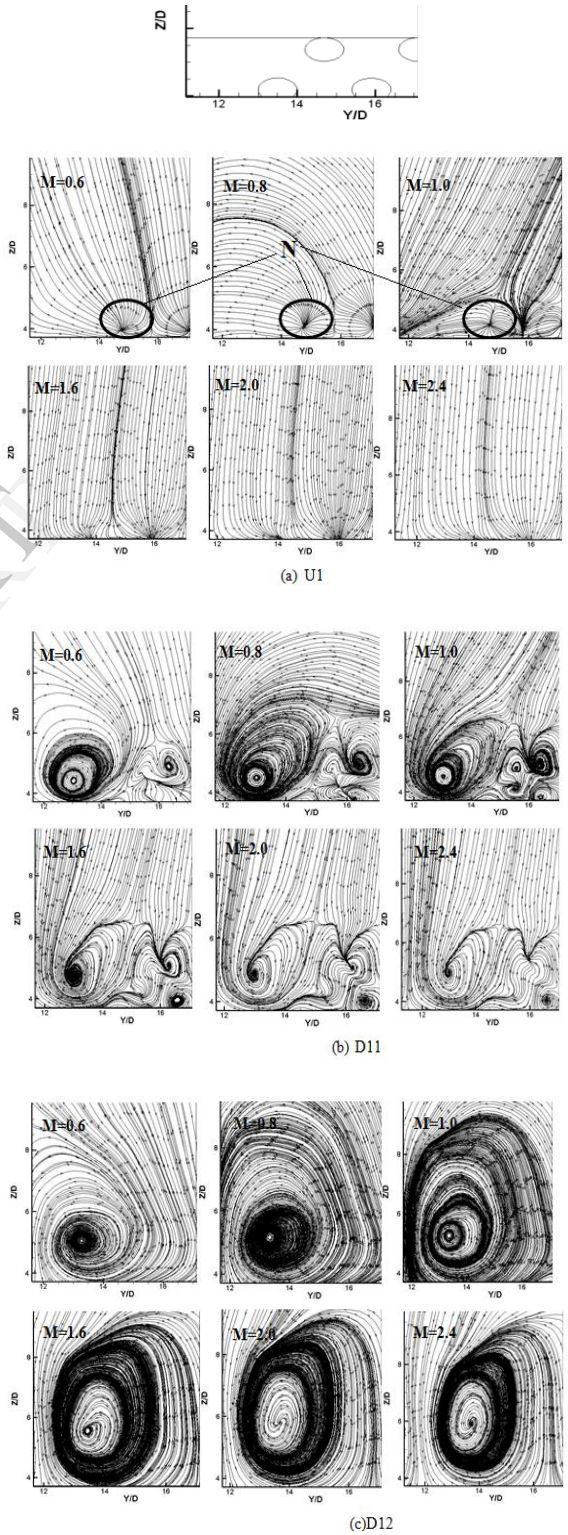

IJERT

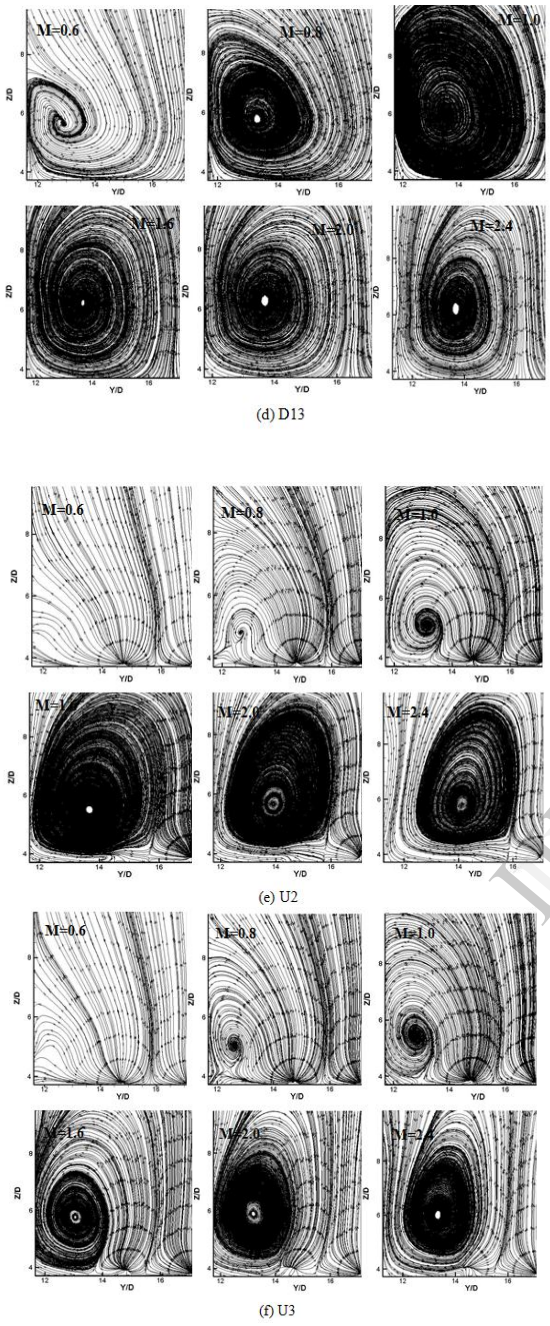

Figure 13. Streamlines for varying blowing ratios at plane (a) U1, (b) D11, (c) D12, (d) D13, (e) U2, (f) U3

6. Conclusion

Adiabatic heat transfer on a flat target plate exposed to hot mainstream and combined impingement and film cooling is investigated computationally. The computational results of temperature distribution on the target surface agree for +8% with the experimental data which is obtained from the Rajesh Kumar Panda and B.V.S.S.S. Prasad [1], because of the adiabatic heat transfer. The predicted results using a 3.6 million mesh are identical to the ones predicted using a 4.2 million mesh. This conclusion permits a significant reduction in the time required to generate the mesh and cost. Also, the results confirm that adiabatic heat transfer models predict a significant difference in the temperature predictions in comparison with the conjugate models.

The SST-k-ω model performs better than the standard k-ε model in predicting the temperature distribution.

The temperature profiles are more uniform. The coolant temperature at film hole exit decreases in the streamwise direction and further reduces with increase in blowing ratio. The lowest blowing ratio provides lowest heat-transfer enhancement. With the increase in blowing ratio, the heat transfer coefficient increases for x/D locations. Minimum heat transfer coefficients are found at medium blowing ratios. When blowing ratio increases, Jet-lift-off increases and it is not aided. It is seen that the boundary layer developed in the wall jet region is removed due to the suction created by the film holes. This boundary layer removal increases the heat transfer. The nodal points of attachment present in the flow structure are responsible for an increase in effectiveness near the leading edge of the holes.

IJERT

10. References

[1] Rajesh Kumar Panda, B.V.S.S.S. Prasad, “Conjugate Heat Transfer from a Flat plate with Combined Impingement and Film cooling”, ASME-TURBO expo, GT2012-68830, Copenhagen, Denmark, June 11-15, 2012.

[2] **C**hougule N.K, Parishwad G.V., Gore P.R, Pagnis S and Sapali S.N,”CFD Analysis of Multi-jet Air Impingement on Flat Plate”, World Congree on Engineering, London, U.K., Vol. III, June 6-8, 2011

[3] Ashok Kumar M., and Prasad, B.V.S.S.S., “Computational flow and heat transfer of Multiple circular jets impinging on a flat surface with effusion holes,” Heat Mass Transfer, Vol. 47, 2011, pp.1121-1132.

[4] Haven, B. A., and Kuroska, M., "Kidney and anti-kidney vortices in cross flow jets", Journal of FluidMechanics, Vol. 352, 1997, pp: 27-64.

[5] Mahmood Silieti, Alain J. Kassab and Eduardo Divo, “ Film cooling effectiveness: Comparison of adiabatic and conjugate heat transfer CFD models”, International Journal of Thermal Sciences, Vol. 48, 2009, pp. 2237-2248.

[6] Siba, E. A., Ganesa-Pillai, M., Harris, K. T. and Haji-Sheikh, A., 2003, “Heat transfer in a high turbulence air jet impinging over a flat circular disk”, ASME Journal of Heat Transfer, Vol. 125, pp: 257-265.

[7] Walters, D. K., and Leylek, J. H., 2000, "A Detailed Analysis of Film-Cooling Physics: Part I—Streamwise Injection With Cylindrical Holes", ASME Journal of Turbomachinery, Vol. 122, pp: 102-112.

[8] Colban, W., Thole, K. A., and Haendler, M., 2007

Experimental and Computational Comparisons of Fan-Shaped Film Cooling on a Turbine Vane Surface, ASMEJournal of Turbomachinery, Vol. 129, pp: 23-31.

[9] Miao, J. M., and Wu, C. Y., 2006, "Numerical approach to hole shape effect on film cooling effectiveness over flat plate including internal impingement cooling chamber", International Journal of Heat and Mass Transfer, Vol. 49, pp: 919–938.

[10] Oh, S. H., Lee, D. H., Kim, K.M, Kim, M. Y, and Cho, H. H., 2008, "Enhanced Cooling Effectiveness in Full-coverage Film Cooling System With impingement Jets", ASME-TurboExpo2008, GT2008-50784, June 9-13, Berlin, Germany.

[11] Jung, Y. E., Lee, D. H., Oh, S. H., Kim K. M., and Cho, H. H., 2010, "Total Cooling Effectiveness on A Staggered Full-Coverage Film Cooling Plate with Impinging Jet", ASME-TurboExpo2010, GT2010-23725, June 14-18, Glasgow, U.K.

IJERT